

Identifying the structure of near-threshold states from the line shape^{*}CHEN Guo-Ying^{1,4)} HUO Wen-Sheng¹⁾ ZHAO Qiang^{2,3)}¹ Department of Physics, Xinjiang University, Urumqi 830046, China² Institute of High Energy Physics, Chinese Academy of Sciences, Beijing 100049, China³ Theoretical Physics Center for Science Facilities, CAS, Beijing 100049, China⁴ State Key Laboratory of Theoretical Physics, Institute of Theoretical Physics, Chinese Academy of Sciences, Beijing 100190, China

Abstract: We revisit the compositeness theorem proposed by Weinberg in an effective field theory (EFT) and explore criteria which are sensitive to the structure of S -wave threshold states. On a general basis, we show that the wave function renormalization constant Z , which is the probability of finding an elementary component in the wave function of a threshold state, can be explicitly introduced in the description of the threshold state. As an application of this EFT method, we describe the near-threshold line shape of the $D^{*0}\bar{D}^0$ invariant mass spectrum in $B \rightarrow D^{*0}\bar{D}^0 K$ and determine a nonvanishing value of Z . It suggests that the $X(3872)$ as a candidate of the $D^{*0}\bar{D}^0$ molecule may still contain a small $c\bar{c}$ core. This elementary component, on the one hand, explains its production in the B meson decay via a short-distance mechanism, and on the other hand, is correlated with the $D^{*0}\bar{D}^0$ threshold enhancement observed in the $D^{*0}\bar{D}^0$ invariant mass distributions. Meanwhile, we also show that if Z is non-zero, the near-threshold enhancement of the $D^{*0}\bar{D}^0$ mass spectrum in the B decay will be driven by the short-distance production mechanism.

Key words: $X(3872)$, effective field theory, compositeness

PACS: 14.40.Lb, 14.40.Rt

1 Introduction

Recently the observations of many new resonances, namely the so-called XYZ states, have initiated intensive studies of their properties in both experiment and theory. An interesting feature about most of these new resonances is that their masses are generally close to S -wave two-particle thresholds and their coupling to the corresponding S -wave two-particle channel is important. For example, the famous $X(3872)$ is one of the earliest observed states correlated to the $D^{*0}\bar{D}^0$ threshold. We use the notation $D^{*0}\bar{D}^0$ to denote both $D^{*0}\bar{D}^0$ and $\bar{D}^{*0}D^0$. The structure of these near-threshold resonances are still under debate and there are various existing theoretical interpretations, which include proposals for treating them as either conventional quark-antiquark states or QCD exotics such as tetraquarks, hybrid states, dynamically generated states or molecular states. In some scenarios, they are treated as mixing states of the above mentioned configurations. It is worth mention-

ing that the recent experimental signals for the charged quarkonium states $Z_b(10610)$ and $Z_b(10650)$ [1] and their analogues in the charmonium sector $Z_c(3900)$ [2–4] and $Z_c(4020/4025)$ [5, 6] appear to be strongly correlated to the thresholds of either $B^{(*)}$ or $D^{(*)}$ pairs. Since most of those newly observed states are in the vicinity of an S -wave open threshold, a theoretical method to distinguish whether such a near-threshold state is an elementary state of overall color singlet or a composite state consisting of open channel hadrons as constituents is thus crucial for our understanding of their nature. Although this issue has been explored for a long time and by many theorists (e.g. one can refer to the early literature of Refs. [7–10] and recent review [11] and references therein), our knowledge about such non-perturbative phenomena is still far from complete.

The aim of this present work is to develop an effective field theory (EFT) approach to identify the structure of the near threshold states and explore its appli-

Received 18 November 2014

^{*} This work is supported, in part, by National Natural Science Foundation of China (Grant Nos. 11147022, 11035006 and 11305137), Chinese Academy of Sciences (KJCX2-EW-N01), Ministry of Science and Technology of China (2009CB825200), DFG and the NSFC (No. 11261130311) through funds provided to the Sino-German CRC 110 “Symmetries and the Emergence of Structure in QCD”, and Doctor Foundation of Xinjiang University (No. BS110104)

1) E-mail: chengy@pku.edu.cn

2) E-mail: uni_xinjiang@sina.com

3) E-mail: zhaoq@ihep.ac.cn

©2013 Chinese Physical Society and the Institute of High Energy Physics of the Chinese Academy of Sciences and the Institute of Modern Physics of the Chinese Academy of Sciences and IOP Publishing Ltd

cation to the structures of the recently discovered XYZ states. In particular, we shall study the $X(3872)$ which, since its first observation by the Belle collaboration in $B^\pm \rightarrow K^\pm \pi^+ \pi^- J/\psi$ [12], has initiated tremendous interest in both experiment and theory. Due to the small mass difference between the measured mass of the $X(3872)$ and the $D^{*0} \bar{D}^0$ threshold, the $X(3872)$ is the best candidate for an S -wave $D^{*0} \bar{D}^0$ molecule [13–19]. However, it has also been recognized that the structure of the $X(3872)$ could be rather profound because its large production rates in the B -factories and at the Tevatron seem to favor a compact structure in its wave function rather than a loosely bound molecular state [20–22]. Taking both the production and decay properties into account, it seems reasonable to identify the $X(3872)$ to be a mixing state between the $J^{PC} = 1^{++} c\bar{c}$ component and the $D^{*0} \bar{D}^0$ component [20, 21]. This scenario can also explain why the $\chi'_{c1} c\bar{c}$ state around 3950 MeV predicted by the single-channel theory is missing in experiment [23]. It is worth noting the recent lattice QCD result that a candidate for the $X(3872)$ about 11 ± 7 MeV below the $\bar{D}^0 D^{*0}$ threshold was identified in a lattice simulation with $m_\pi = 266(4)$ MeV [24]. It was also shown that the pion mass dependence of the binding energy can provide important information on the structure of the $X(3872)$ [25–27].

Obviously, more experimental data and theoretical development are required to clarify the nature of the $X(3872)$. Very recently the LHCb collaboration found evidence for the decay mode $X(3872) \rightarrow \psi(2S)\gamma$ in $B^+ \rightarrow X(3872)K^+$. The measured ratio of the branching fraction of $X(3872) \rightarrow \psi(2S)\gamma$ to that of $X(3872) \rightarrow J/\psi\gamma$ is $R_{\psi\gamma} = \frac{\mathcal{B}(X(3872) \rightarrow \psi(2S)\gamma)}{\mathcal{B}(X(3872) \rightarrow J/\psi\gamma)} = 2.46 \pm 0.64 \pm 0.29$ [28]. Such a large value for $R_{\psi\gamma}$ does not support a pure $D^{*0} \bar{D}^0$ molecular interpretation of the $X(3872)$, because $R_{\psi\gamma}$ is predicted to be rather small for a pure $D^{*0} \bar{D}^0$ molecular [29].

Since the pure molecular interpretation of the $X(3872)$ is not favoured, it is then important to study quantitatively how large the compact component is in the wave function of the $X(3872)$. This is the main subject of this study. By analyzing the compositeness relation proposed by Weinberg in the effective field theory, we will establish the relation between experimental observable and the wave function renormalization constant Z such that the hadron structure information encoded in Z can be probed via the measurement of some of those sensitive observables. Specifically, we will show that the line shape of $D^{*0} \bar{D}^0$ in $B \rightarrow X(3872)(\rightarrow D^{*0} \bar{D}^0)K$ could be useful for shedding important light on the structure of the $X(3872)$, see also a recent study in Ref. [30].

2 Weinberg's compositeness theorem in EFT

To proceed, we first give a short review of Weinberg's method to evaluate the coupling constant between a near-threshold state and its two-particle channel [8, 9]. Without losing generality, a total Hamiltonian H of interest can be split into a free part H_0 and an interaction part V to an open channel near the threshold:

$$H = H_0 + V. \quad (1)$$

The eigenstates of the free part H_0 include the continuum states $|\alpha\rangle$ and the possible discrete bare elementary particle states $|n\rangle$, with

$$\begin{aligned} H_0|\alpha\rangle &= E(\alpha)|\alpha\rangle, & \langle\beta|\alpha\rangle &= \delta(\beta - \alpha), \\ H_0|n\rangle &= E_n|n\rangle, & \langle\alpha|n\rangle &= 0, & \langle m|n\rangle &= \delta_{m,n}, \end{aligned} \quad (2)$$

where the energies are defined relative to the two-particle threshold throughout this paper. The completeness relation for the eigenstates of H_0 reads

$$1 = \sum_n |n\rangle\langle n| + \int d\alpha |\alpha\rangle\langle\alpha|. \quad (3)$$

A physical bound state $|d\rangle$ is a normalized eigenstate of the total Hamiltonian H , with

$$H|d\rangle = -B|d\rangle, \quad \langle d|d\rangle = 1, \quad (4)$$

where $B > 0$ is the binding energy. We call $|d\rangle$ a physical bound state in the sense that it has the two open channel particles as constituents in its wavefunction and its mass is below the two-particle threshold or equally, $B > 0$. With the completeness relation in Eq. (3) and the normalization of $|d\rangle$ we can have

$$1 = Z + \int d\alpha |\langle\alpha|d\rangle|^2, \quad Z \equiv \sum_n |\langle n|d\rangle|^2, \quad (5)$$

where Z is the probability of finding an elementary state in the physical bound state. Hence $Z = 0$ indicates that the physical bound state is purely composite, while $0 < Z < 1$ indicates that there also exists an elementary component inside the physical state. The determination of the value of Z would thus enable us to distinguish a pure composite state from a mixture of a composite and elementary configuration.

With the relation $|d\rangle = [H - H_0]^{-1}V|d\rangle$ and Eqs. (2) and (4), we can obtain

$$\begin{aligned} \langle\alpha|d\rangle &= \langle\alpha|[H - H_0]^{-1}V|d\rangle \\ &= -\frac{\langle\alpha|V|d\rangle}{E(\alpha) + B}. \end{aligned} \quad (6)$$

Then, Eq. (5) can be written as

$$1 - Z = \int d\alpha \frac{|\langle\alpha|V|d\rangle|^2}{(E(\alpha) + B)^2}. \quad (7)$$

For small B , the above integral nearly diverges, so it can then be approximately evaluated by restricting $|\alpha\rangle$ to low-energy two-particle states. If the coupling between $|d\rangle$ and the two-particle state is an S -wave coupling, we can then replace $|\langle\alpha|V|d\rangle|$ by g , and replace the α integral with

$$d\alpha = \frac{4\pi p^2 dp}{(2\pi)^3} = \frac{\mu^{3/2}}{\sqrt{2\pi^2}} E^{1/2} dE, \quad E \equiv p^2/2\mu, \quad (8)$$

where μ is the reduced mass of the two constituents. After these replacements we then obtain the effective coupling constant

$$g^2 = \frac{2\pi\sqrt{2\mu B}}{\mu^2}(1-Z), \quad (9)$$

which encodes the structure information of the composite system [31]. Notice that our definition for g^2 has a relative factor $(2\pi)^3$ compared with that in Ref. [9]. We use this convention, because this make it convenient to incorporate the compositeness theorem in the EFT approach.



Fig. 1. Feynman diagrams for the two particle scattering. The double line denotes the bare state.

Now we will incorporate the compositeness theorem in the EFT approach. Consider a bare state $|\mathcal{B}\rangle$ with bare mass $-B_0$ and coupling g_0 to the two-particle state. If $|\mathcal{B}\rangle$ is near the two-particle threshold, then the leading two-particle scattering amplitude can be obtained by summing the Feynman diagrams in Fig. 1. Later, we will provide a power counting argument to justify the summation. Near threshold, the momenta of these two particles are non-relativistic. Therefore, the loop integral in Fig. 1 can be done the same way as that in Ref. [32, 33]. With the minimal subtraction (MS) scheme, the result of the loop integral can be written as

$$\begin{aligned} \mathcal{I}^{MS} &\equiv \int \frac{d^D \ell}{(2\pi)^D} \frac{i}{[\ell^0 - \vec{\ell}^2/(2m_1) + i\epsilon]} \\ &\quad \times \frac{i}{[E - \ell^0 - \vec{\ell}^2/(2m_2) + i\epsilon]} \\ &= i \frac{\mu}{2\pi} \sqrt{-2\mu E - i\epsilon}. \end{aligned} \quad (10)$$

Thus, the Feynman amplitude for Fig. 1 reads

$$\mathcal{A} = -\frac{g_0^2}{E + B_0 - g_0^2 \frac{\mu}{2\pi} \sqrt{-2\mu E - i\epsilon}}. \quad (11)$$

Because a physical bound state $|d\rangle$ corresponds to a pole at $E = -B$, we have

$$B_0 - g_0^2 \frac{\mu}{2\pi} \sqrt{2\mu B} \equiv B, \quad \Rightarrow \quad B_0 = B + g_0^2 \frac{\mu}{2\pi} \sqrt{2\mu B}. \quad (12)$$

Then, the amplitude can be written as

$$\mathcal{A} = \frac{\delta'}{E + B + \tilde{\Sigma}'(E)}, \quad (13)$$

where $\delta' = -\frac{g_0^2}{1 + g_0^2 \mu^2 / (2\pi\sqrt{2\mu B})}$ is the residual of the bound state pole, and

$$\tilde{\Sigma}'(E) = \delta' \left[\frac{\mu}{2\pi} \sqrt{-2\mu E - i\epsilon} + \frac{\mu\sqrt{2\mu B}}{4\pi B} (E - B) \right]. \quad (14)$$

Since δ' is the residual of the bound state pole, it naturally leads to the connection of $\delta' \equiv -g^2$ where g^2 is defined in Eq. (9) as the effective coupling constant. Therefore, the leading order amplitude for the two-particle scattering can be written as

$$\mathcal{A} = -\frac{g^2}{E + B + \tilde{\Sigma}'(E)}, \quad (15)$$

where $\tilde{\Sigma}'(E)$ can now be written as

$$\tilde{\Sigma}'(E) = -g^2 \left[\frac{\mu}{2\pi} \sqrt{-2\mu E - i\epsilon} + \frac{\mu\sqrt{2\mu B}}{4\pi B} (E - B) \right]. \quad (16)$$

One can easily check that the amplitude given in Eq. (15) satisfies the unitary condition. Actually, the same solution as Eq. (15) was obtained by Weinberg fifty years ago, but with a different approach [9]. With $\delta' = -g^2$ and Eq. (9), we obtain

$$g_0^2 = \frac{2\pi\sqrt{2\mu B}}{\mu^2} \frac{1-Z}{Z} = g^2/Z. \quad (17)$$

Combining Eq. (12) and (17) together we obtain

$$B_0 = \frac{2-Z}{Z} B. \quad (18)$$

The limit $B_0 \rightarrow \infty$ corresponds to $Z \rightarrow 0$, which is consistent with the condition discussed in [8]. Also, Eq. (17) defines the wave function renormalization constant of $|\mathcal{B}\rangle$, i.e. $Z = 1/[1 + g_0^2 \mu^2 / (2\pi\sqrt{2\mu B})]$, which is the same as the result in Ref. [34]. Comparing Eq. (15) with the effective range expansion formula

$$\mathcal{A} = \frac{2\pi}{\mu} \frac{1}{-1/a + \frac{1}{2} r_0 p^2 - ip + \mathcal{O}(p^4)}, \quad (19)$$

we have the famous relations which were first obtained by Weinberg [9]

$$a = \frac{2(1-Z)}{2-Z} \frac{1}{\sqrt{2\mu B}}, \quad r_0 = -\frac{Z}{1-Z} \frac{1}{\sqrt{2\mu B}}, \quad (20)$$

where a is the scattering length and r_0 is the effective range.

It is interesting to examine the behavior of the tree diagram amplitude in Fig. 1 near threshold. The tree diagram amplitude reads

$$\mathcal{A}_{tree} = -\frac{g_0^2}{E+B_0}. \quad (21)$$

In the limit $Z \rightarrow 0$, we have $B_0 \rightarrow \infty$ and $g_0 \rightarrow \infty$. However, \mathcal{A}_{tree} is still well defined. With Eqs. (17) and (18), we have

$$\lim_{Z \rightarrow 0} \mathcal{A}_{tree} = -\frac{2\pi}{\mu\sqrt{2\mu B}}. \quad (22)$$

Equation (22) is just the equivalence of the four-Fermi theory and Yukawa theory found in Ref. [10]. To be explicit, in the limit $Z \rightarrow 0$, the S -channel resonance exchange interaction will reduce to the contact interaction. Since we are interested in the low energy physics, the binding momentum $\gamma = (2\mu B)^{1/2}$ and the three-momentum of the two-particle state p is small. We can count these two momenta as the same order, i.e. $\gamma, p \sim \mathcal{O}(p)$. One can see that due to the existence of the bound state the coefficient of the leading contact term can be enhanced to the order of $(2\mu B)^{-1/2} \sim \mathcal{O}(p^{-1})$. Hence in such a case all the bubble diagrams of the leading contact term are equally important and should be resummed at the leading order. It is straightforward to apply this power counting argument to the case $Z \neq 0$. One then find that all the Feynman diagrams in Fig. 1 are at the same order of $\mathcal{O}(p^{-1})$, therefore they should be resummed. A similar power counting argument to support the summation of the leading contact term is provided in Ref. [32, 33], in which a new subtraction scheme i.e. power divergence subtraction (PDS) scheme, is proposed. If we use the PDS scheme, then Eq. (11) will become

$$\mathcal{A}_{PDS} = -\frac{g_0^2}{E+B_0 - g_0^2 \frac{\mu}{2\pi} (\sqrt{-2\mu E - i\epsilon} - \Lambda_{PDS})}, \quad (23)$$

where Λ_{PDS} is the dimensional regularization parameter. By extracting the bare mass similar to what we have done above, we find that Eqs. (15)–(17) still hold but Eq. (18) will be changed to

$$B_0 = \frac{2-Z}{Z}B - \frac{1-Z}{Z}\sqrt{2B/\mu}\Lambda_{PDS}. \quad (24)$$

If $Z \neq 0$ and $Z \neq 1$, the bare mass B_0 determined from Eq. (24) will depend on the regularization parameter Λ_{PDS} , which can be arbitrary. It means that the determination of the bare mass will inevitably depend on the scheme as emphasized in Ref. [35]. As a consequence, one presumably need not worry too much about the physical meaning of a bare mass. In contrast, the physical observable such as Eq. (15) is scheme-independent and can be determined by measuring the line shape.

In the above, we have incorporated the compositeness theorem in the EFT, and we obtain the leading order amplitude for the low energy S -wave two-particle scattering when a bound state exists, which is given in Eq. (15). It is interesting and important to compare the amplitude with other low energy amplitudes which are widely used in studying the structure of the XYZ states. In Refs. [36, 37], the authors use the following low energy amplitude

$$f(E) = \frac{1}{-1/a + \sqrt{-2\mu E - i\epsilon}}, \quad (25)$$

One can find that $f(E)$ is just the amplitude given in Eq. (19) if the term $\frac{1}{2}r_0 p^2$ is neglected. From Eq. (20), one can find that if $Z = 0$, then $r_0 = 0$, and the term $\frac{1}{2}r_0 p^2$ disappears in the amplitude. However, if $Z \neq 0$, $\frac{1}{2}r_0 p^2$ is at the order of $\mathcal{O}(p)$, which is the same as the term $\sqrt{-2\mu E - i\epsilon}$ or $-ip$. Therefore the term $\frac{1}{2}r_0 p^2$ cannot be neglected in the low energy amplitude for $Z \neq 0$. This suggests that $f(E)$ can only be used if a bound state is a pure molecule.

In Refs. [38–40], the authors use the Flatté parametrization for the low energy amplitude. Considering only the single channel coupling, the Flatté amplitude reads

$$F(E) = -\frac{1}{2} \frac{g_1}{E - E_f - \frac{1}{2}g_1\sqrt{-2\mu E - i\epsilon} + i\frac{1}{2}\Gamma}. \quad (26)$$

Neglecting Γ , one can find that $F(E)$ is essentially the same as our amplitude given in Eq. (11). By comparing $F(E)$ with Eq. (11), one can find that

$$g_1 = g_0^2\mu/\pi, \quad E_f = -B_0. \quad (27)$$

With Eq. (17) and Eq. (18), one can realize that $F(E)$ can only be applied if Z is not very small, or the bound state contains a substantial compact component, because in the limit $Z \rightarrow 0$, the Flatté parameters g_1 and E_f become infinite. In such a case the fitting with Flatté parametrization will exhibit scaling behavior as was found in Ref. [39]. Therefore, if $Z \rightarrow 0$, in order to obtain the parameters of the near threshold state, one had better use $F(E)$ in the form that both the numerator and denominator are multiplied by a factor Z . One can easily find that in such form $F(E)$ is just $f(E)$, which is given in Eq. (25). In short, $f(E)$ can only be applied if the bound state is purely dynamically generated or $Z = 0$, and $F(E)$ can only be applied if the bound state contains a substantial compact component. In contrast, the low energy amplitude given in Eq. (15) can be used in both cases, and in the study of the XYZ states, it is better to use the amplitude given in Eq. (15).

3 Study of the $X(3872)$ in the EFT approach

We show how to incorporate Weinberg's compositeness theorem in the EFT and apply it to the study of threshold states in which both elementary and molecular configurations could be present. Although most of the formulae we present above had been obtained with the quantum mechanical approach [9, 31], it is still useful to reproduce them in the EFT approach. The idea is that with the EFT, we can obtain the relevant Feynman rules for the near-threshold states. These Feynman rules can then be directly applied to processes involving such states as a more realistic prescription for their threshold behaviors. What is more important is that with the EFT approach, we can set up the power counting and study the higher order corrections systematically. Therefore the EFT approach can be applied much more easily to phenomenological studies and may provide a clearer physical picture for some of those threshold states. We also mention that some of those points have been addressed or demonstrated in the recent analyses of Refs. [41–43].

In the following, as an application we will use the EFT approach to study the structure of the $X(3872)$. Before proceeding, we would like to clarify that our approach for the $X(3872)$ is different from the XEFT approach [44] where the $X(3872)$ is assumed to be a weakly bound molecule of the $D^{*0}\bar{D}^0$ pair. This corresponds to the special case with $Z = 0$ in the EFT approach. Instead, we do not make any assumption on the structure of the $X(3872)$ in advance, i.e. we leave the Z as a free parameter which can be determined by the physical observables.

First, we give the relevant Feynman rules for the $X(3872)$ in our EFT approach. The propagator of the $X(3872)$ is

$$G(E)_X = \frac{iZ}{E + B + \bar{\Sigma}'(E) + i\Gamma/2}, \quad (28)$$

where Γ denotes the width of the $X(3872)$ which comes from the decay modes that do not proceed through its $D^{*0}\bar{D}^0$ component. Our convention is that a factor of $\sqrt{2M_X}$ has been absorbed into the field operator of the $X(3872)$. It is convenient to use this convention for the boson in the nonrelativistic formalism. Hence a boson field has the dimension of 3/2 and the Feynman rule for an external boson should be $\sqrt{2M}$. Actually, the coupling constant g^2 in Eq. (9) is defined under this convention. The Feynman rule for the $XD^{*0}\bar{D}^0$ coupling is given as

$$i\frac{g_0}{\sqrt{2}} = i\left(\frac{g^2}{2Z}\right)^{1/2}, \quad (29)$$

where the factor $1/\sqrt{2}$ is due to the definition of the

C -even state $(D^{*0}\bar{D}^0 + D^0\bar{D}^{*0})/\sqrt{2}$.

As mentioned before, near threshold, there are two small momenta, the binding momentum $\gamma = (2\mu B)^{1/2}$ and the three momentum of the charmed meson p . We can count these two momenta as the same order, i.e. $\gamma, p \sim \mathcal{O}(p)$. Therefore, we can find that $E, B \sim \mathcal{O}(p^2)$ and $g \sim \mathcal{O}(p^{1/2})$. One can then easily check that the elastic scattering amplitude given in Eq. (15) is at the order of $\mathcal{O}(p^{-1})$ which is consistent with the result in Ref. [32, 33].

Now we come to describe the line shape of $D^{*0}\bar{D}^0$ in $B \rightarrow X(3872)K \rightarrow D^{*0}\bar{D}^0K$ in this EFT approach. For studies of the line shape with other approaches one can refer to Refs. [36–40]. In Ref. [36, 37], the authors use the amplitude $f(E)$ which is given in Eq. (25) in their analysis. As we have mentioned before, $f(E)$ can only be used for a pure molecule. However, a pure molecule assignment for the $X(3872)$ seems to conflict with the recent LHCb measurement [28]. In Refs. [38–40], the authors describe the $D^{*0}\bar{D}^0$ line shape with Flatté parametrization. Assuming the $X(3872)$ production via the short-distance process, Ref. [40] further addresses the question of a possible χ'_{c1} charmonium admixture in the wave function of the $X(3872)$. The idea is to integrate the spectral density which can be expressed in terms of Flatté parameters. However, in this approach the integration bounds are somewhat arbitrary, hence this approach is inevitably model dependent. Comparing with these approaches, the advantage of our approach is that we make no assumptions on the structure of the $X(3872)$ in advance. In this way, one can then clearly address the question whether a bound state is a pure molecule or it contains a substantial compact component. Another advantage of our approach is that instead of making assumptions on the production mechanism of the $X(3872)$ as in Ref. [38–40], we systematically consider both the short and long-distance production mechanisms of the $X(3872)$. In the short-distance production mechanism the $X(3872)$ is produced directly at the short-distance vertex of the B decay, while in the long-distance production mechanism a $D^{*0}\bar{D}^0$ pair is produced first in the B decay and then rescatters into the $X(3872)$. The answer to the question about which production mechanism is more important than the other would depend on the structure of the $X(3872)$. As follows, instead of making assumptions on the structure of the $X(3872)$ in advance, we actually consider both these different production mechanisms in our analysis.

The leading order Feynman diagrams for these two different production mechanisms are presented in Fig. 2, for which the Feynman amplitudes can be explicitly expressed as

$$i\mathcal{M}_a = -\frac{A_{XK}}{\sqrt{2}} \frac{\sqrt{Z}g}{E + B + \bar{\Sigma}'(E) + i\Gamma/2} \vec{p}_K \cdot \vec{\epsilon}^*,$$

$$i\mathcal{M}_b = \mathcal{B}_{DDK} \frac{\mu}{2\pi} \frac{g^2 \sqrt{-2\mu E - i\epsilon}}{E + B + \tilde{\Sigma}'(E) + i\Gamma/2} \vec{p}_K \cdot \vec{\epsilon}^*, \quad (30)$$

where p_K is the momentum of the K meson in the rest frame of the B meson, and ϵ is the polarization vector of the outgoing D^{*0} . We use \mathcal{A}_{XK} and \mathcal{B}_{DDK} to denote the first production vertices in Fig. 2, i.e. $B \rightarrow X(3872)K$ and $B \rightarrow D^{*0}\bar{D}^0K$, respectively. Near the threshold of $D^{*0}\bar{D}^0$, we can treat \mathcal{A}_{XK} and \mathcal{B}_{DDK} as constants. Note that we have omitted the factors from the external $D^{(*)}$ mesons in Eq. (30) which can be absorbed into \mathcal{A}_{XK} and \mathcal{B}_{DDK} .

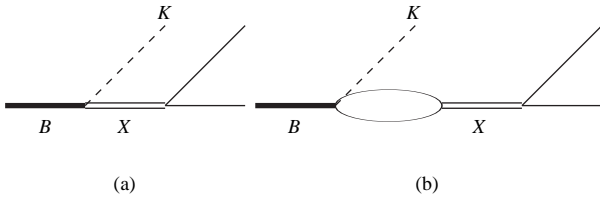


Fig. 2. Feynman diagrams for $B \rightarrow X(3872)K \rightarrow D^{*0}\bar{D}^0K$. Solid lines in the loop and final state represent the charm and anti-charm mesons.

It is easy to count the power of the above amplitudes and one can find $\mathcal{M}_a \sim \mathcal{O}(p^{-3/2})$ and $\mathcal{M}_b \sim \mathcal{O}(p^0)$. From the power counting, one may find that the short-distance production mechanism is more important than the long-distance one. However, it should be noted that \mathcal{M}_a is proportional to the factor \sqrt{Z} . Therefore, its contribution will be suppressed if the $X(3872)$ is dominated by a molecular component. It is interesting to note that with $Z=0$ the term of \mathcal{M}_a will vanish, and then the production of the $X(3872)$ will only come from the long-distance production mechanism \mathcal{M}_b . This feature ensures that our separation of the short-distance production mechanism from the long-distance one makes sense.

Taking into account the non-resonance production contribution, the full amplitude to describe $B \rightarrow D^{*0}\bar{D}^0K$ is expressed as

$$i\mathcal{M} = i\mathcal{M}_a + i\mathcal{M}_b + \mathcal{B}_{DDK} \vec{p}_K \cdot \vec{\epsilon}^*(D^*), \quad (31)$$

where the term $\mathcal{B}_{DDK} \vec{p}_K \cdot \vec{\epsilon}^*(D^*)$ describes the non-resonance production which is at the same order as $i\mathcal{M}_b$. Now we can use the above amplitude to describe the Belle and BaBar data [45, 46]. The free parameters in our calculation include Γ , B , Z , \mathcal{A}_{XK} and \mathcal{B}_{DDK} . However, the experimental data have large error bars. To reduce the uncertainty, we fix Γ and B with the values that are determined in $X(3872) \rightarrow J/\psi X$, where X denotes the light hadrons. The reason is because the data from the decay modes of $X(3872) \rightarrow J/\psi X$ have higher statistics and there the $X(3872)$ appears as a narrow Breit-Wigner structure. We adapt the PDG [47] value $M_{X(3872)} = 3871.68$ MeV for the mass of $X(3872)$, which

is the average over the measurements from the decay modes of $X(3872) \rightarrow J/\psi X$. With $M_{D^{*0}} = 2006.99$ MeV and $M_{\bar{D}^0} = 1864.86$ MeV [47], we can fix the binding energy as $B = 0.17$ MeV. The width of $X(3872)$ is not settled by the data for $X(3872) \rightarrow J/\psi X$, but the upper limit is given as $\Gamma < 1.2$ MeV. Since the width is small, we fix the non- $D^{*0}\bar{D}^0$ width $\Gamma = 0$ in our fitting. We have checked that the $D^{*0}\bar{D}^0$ line shape is not sensitive to B and Γ around the fixed values. Therefore, our fitting parameters are \mathcal{A}_{XK} , \mathcal{B}_{DDK} and Z .

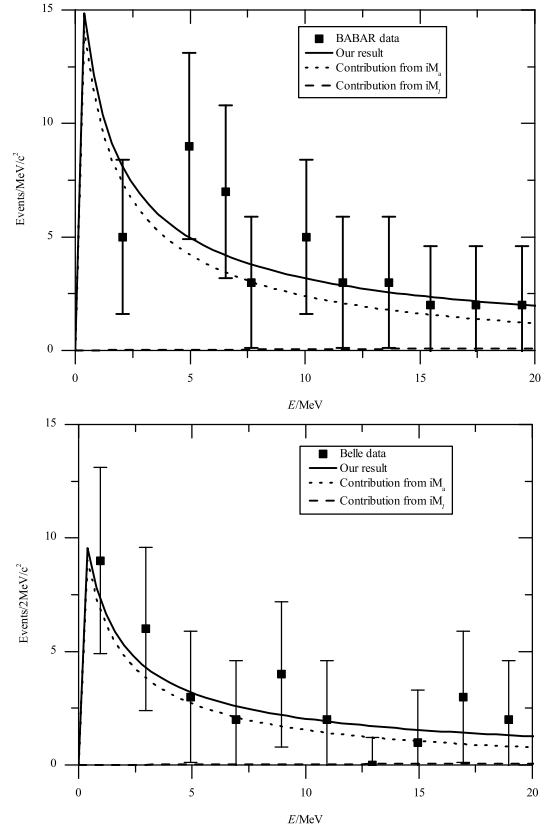


Fig. 3. The line shape of the $D^{*0}\bar{D}^0$ spectrum in $B \rightarrow D^{*0}\bar{D}^0K$. The data are from Refs. [45, 46]. The solid line denotes the overall fitting result, the dotted line is the contribution from $i\mathcal{M}_a$, and the dashed line that from $i\mathcal{M}_\ell = i\mathcal{M}_b + \mathcal{B}_{DDK} \vec{p}_K \cdot \vec{\epsilon}^*(D^*)$. An arbitrary normalization is implemented.

The fitting results are presented in Fig. 3 and compared with the experimental data [45, 46]. Notice that there is an arbitrary scaling factor between the BABAR and Belle data; we fit the ratio $\mathcal{A}_{XK}/\mathcal{B}_{DDK}$ and Z for these two sets of data simultaneously but leave a free scale factor to be fitted by the data. This, in principle, introduces an additional parameter and leads to $\chi^2/d.o.f = 0.4$ which indicates some correlations among the parameters. This can be improved by future experimental measurement. For the physical discussion, we

only list the fitted ratio $\mathcal{A}_{XK}/\mathcal{B}_{DDK}$ and parameter Z as follows

$$\frac{\mathcal{A}_{XK}}{\mathcal{B}_{DDK}} = -0.15 \pm 0.65 \text{ GeV}^{3/2}, \quad Z = 0.19 \pm 0.29. \quad (32)$$

In Fig. 3, we also show the contribution from different pieces of the amplitude, i.e. $i\mathcal{M}_a$ and $i\mathcal{M}_\ell = i\mathcal{M}_b + \mathcal{B}_{DDK}\vec{p}_K \cdot \vec{\epsilon}^*(D^*)$ as the dotted and dashed line, respectively. From Eq. (32) one can see that the fitted parameters are with large uncertainties due to the large error bars with the BABAR and Belle data. To reduce the number of the free parameters one can only use the leading order amplitude $i\mathcal{M}_a$ in the fitting. The fitted Z is $Z = 0.12 \pm 0.11$. The fitting quality is almost the same as that of Eq. (32). Because the fitting line shape is similar to that in Fig. 3, we will not bother to show it again.

Due to the relatively large uncertainties with the fitted parameters, we discuss the following possible scenarios arising from the fitting results:

- The main feature of Fig. 3 is that a small nonvanishing value of Z will result in a sizeable contribution from the short-distance process, i.e. $i\mathcal{M}_a$. This indicates that the production of the $X(3872)$ in the B decay is driven by the short-distance production mechanism. Even a small component of the $c\bar{c}$ core will lead to a relatively larger production rate for the $X(3872)$ in comparison with when it is treated as a pure $D^{*0}\bar{D}^0$ molecule. Nevertheless, the dominance of the short-distance production mechanism seems to always produce the threshold enhancement which may bring concerns about the molecular feature of the $X(3872)$. However, this may provide a natural explanation for the sizeable production rate for the $X(3872)$ in the B decay, and also explain the large isospin violations given that the compact $c\bar{c}$ component can couple strongly to the charged $D^*\bar{D}+c.c.$ pair. This will give rise to enhanced isospin violation transitions into $J/\psi\rho$ via the intermediate charged and neutral D meson loops as discussed in the literature. If the compact component of the $X(3872)$ is χ'_{c1} , its production rate in the B decay should be comparable with that of χ_{c1} [20]. Meanwhile, if the $X(3872)$ is a pure molecule, its production rate will be strongly suppressed. The recent PDG result gives $\text{Br}(B^+ \rightarrow \chi_{c1}K^+) = (4.79 \pm 0.23) \times 10^{-4}$, while the production ratio of the $X(3872)$ is constrained as $\text{Br}(B^+ \rightarrow X(3872)K^+) < 3.2 \times 10^{-4}$ [47]. Thus, it is not conclusive for the structure of the $X(3872)$ based on such a measurement. We expect that a more precise measurement of the decay rate of $B \rightarrow X(3872)K$ would provide a quantitative constraint on the $X(3872)$ structure in the future.

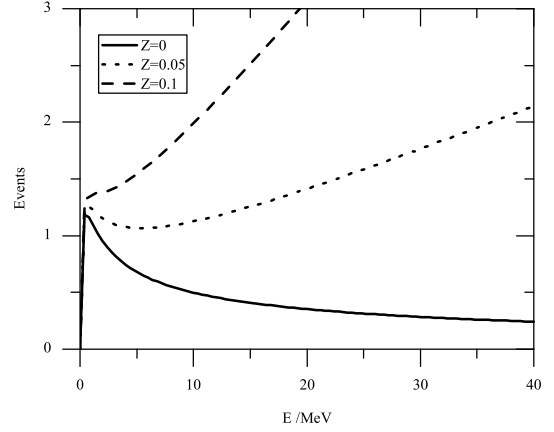


Fig. 4. The exclusive contribution from $i\mathcal{M}_\ell$ to the line shape of the $D^{*0}\bar{D}^0$ spectrum in $B \rightarrow D^{*0}\bar{D}^0K$ with different Z . Here, we set $B = 0.5$ MeV as an illustration. The results with $B = 0.17$ MeV are similar. An arbitrary normalization is implemented.

- It is interesting to discuss the behavior of the term $i\mathcal{M}_\ell$ in the line shape of $D^{*0}\bar{D}^0$. In the case where the $X(3872)$ is a pure molecule, i.e. $Z = 0$, the line shape will be determined by $i\mathcal{M}_\ell$ with $i\mathcal{M}_a = 0$. For convenience, we can express $i\mathcal{M}_\ell$ by a more compact form

$$\begin{aligned} i\mathcal{M}_\ell &= i\mathcal{M}_b + \mathcal{B}_{DDK}\vec{p}_K \cdot \vec{\epsilon}^*(D^*) \\ &= \mathcal{B}_{DDK} \frac{ZE + (2-Z)B}{E + B + \tilde{\Sigma}'(E)} \vec{p}_K \cdot \vec{\epsilon}^*(D^*), \end{aligned} \quad (33)$$

where we have set $\Gamma = 0$ as discussed above. By setting $Z = 0$ the energy dependence of \mathcal{M}_ℓ is just the same as $f(E)$, which is used in Ref. [36, 37]. As discussed before, if we fix $Z = 0$, these two approaches should indeed converge as expected. However, the explicit Z -dependence will bring novel aspects to the line shape description.

We can take a closer look at the Z -dependence of $i\mathcal{M}_\ell$, which is illustrated by the line shape in Fig. 4. Note that Fig. 4 is rescaled by an arbitrary factor due to the unknown value of the cross sections. One can see that the line shape is very sensitive to Z . If $Z = 0$, the line shape has a clear near-threshold enhancement. But when Z increases, the near-threshold enhancement disappears quickly. The reason is that if $Z \neq 0$ the factor ZE in the numerator of Eq. (33) will play an important role in the line shape. From Eq. (33) one can also find that, for $Z = 0$, $i\mathcal{M}_\ell$ is proportional to the small binding energy B . Therefore, we can conclude that if Z is non-negligible, the near-threshold enhancement of the $D^{*0}\bar{D}^0$ mass spectrum in the B decay will be driven by the short-distance production mechanism of the $X(3872)$, although the

dominant component of the $X(3872)$ is molecular. This feature is again consistent with the success of treating the $X(3872)$ as pure molecule in the explanation of the line shape [36, 37]. One should note that even if the long-distance production is enhanced by some unexpected mechanism, the conclusion is still true.

- One may consider to further describe the line shape measured from $X(3872) \rightarrow J/\psi\pi^+\pi^-$ [48, 49] in order to have a better determination of Z . However, since the coupling between $X(3872)$ and $J/\psi\pi^+\pi^-$ is unclear, namely, they may couple directly or through the intermediate meson loops, the inclusion of the line shape measured in $X(3872) \rightarrow J/\psi\pi^+\pi^-$ will inevitably introduce more free parameters. This will be studied in the future with the availability of more precise experimental data.
- In obtaining the above amplitudes, the MS scheme is adopted to evaluate the loop integral. It is still interesting to discuss the results when the PDS scheme is adopted. With the PDS scheme, the amplitude \mathcal{M}_a remains the same but the amplitude \mathcal{M}_ℓ will change to

$$i\mathcal{M}_\ell = \mathcal{B}_{DDK} \times \vec{p}_K \cdot \vec{\epsilon}^* \times \frac{ZE + (2-Z)B - (1-Z)\sqrt{2B/\mu}\Lambda_{PDS}}{E + B + \tilde{\Sigma}'(E)}. \quad (34)$$

If $Z=0$, the arbitrary scale Λ_{PDS} can be absorbed into the definition of \mathcal{B}_{DDK} to make sure that the physical amplitude \mathcal{M}_ℓ does not depend on this arbitrary scale. However, if $0 < Z < 1$, it seems impossible to do that due to the factor ZE in the numerator. Therefore, for $0 < Z < 1$ the amplitude \mathcal{M}_ℓ will inevitably depend on the arbitrary scale Λ_{PDS} if the PDS scheme is adopted. Whether this

means that the PDS scheme may not be suitable for the study of the decay processes in our EFT needs to be further investigated. We note that the same problem does not occur in two-particle elastic scattering in the EFT approach as discussed before.

4 Summary

In summary, we have proposed an EFT approach with the compositeness theorem incorporated for the study of threshold states. By determining Z , which is the probability of finding an elementary component in the bound state via physical observables, our EFT approach can be used to identify the structure of the S -wave near-threshold states. As an example of the application, we use the EFT approach to describe the line shape of the $D^{*0}\bar{D}^0$ mass spectrum in the decay of $B \rightarrow D^{*0}\bar{D}^0 K$. By fitting the data from BaBar and Belle, we obtain a nonvanishing value of $Z = 0.19 \pm 0.29$. Although higher statistics data for $B \rightarrow X(3872)(\rightarrow D^{*0}\bar{D}^0)K$ are needed to reduce the uncertainty of Z , the study of the Z dependence of the transition amplitudes suggests that a small value of Z inside the $X(3872)$ would cause the threshold enhancement in the $D^{*0}\bar{D}^0$ invariant mass spectrum via the short-distance production mechanism. It alternatively implies that the $X(3872)$ is dominated by the molecular $D^{*0}\bar{D}^0$ molecular component. This scenario can naturally explain the observation of sizeable isospin violation decays of $X(3872) \rightarrow J/\psi\rho^0$ via the charged and neutral $D^*\bar{D} + c.c.$ meson loops as the leading contribution. Finally, it will be very interesting to constrain Z from other approaches. For example, in Ref. [50] the determined value of Z is $Z = (28 - 44)\%$, which is close to our result.

We would like to thank Hanqing Zheng and Christoph Hanhart for valuable discussions and suggestions.

References

- 1 Bondar A et al. (Belle Collaboration). Phys. Rev. Lett., 2012, **108**: 122001
- 2 Ablikim M et al. (BESIII Collaboration). Phys. Rev. Lett., 2013, **110**: 252001
- 3 Liu Z Q et al. (Belle Collaboration). Phys. Rev. Lett., 2013, **110**: 252002
- 4 Xiao T, Dobbs S, Tomaradze A et al. Phys. Lett. B, 2013, **727**: 366
- 5 Ablikim M et al. (BESIII Collaboration). Phys. Rev. Lett., 2013, **111**: 242001
- 6 Ablikim M et al. (BESIII Collaboration). Phys. Rev. Lett., 2014, **112**: 022001
- 7 Salam A. Nuovo Cim., 1962, **25**: 224
- 8 Weinberg S. Phys. Rev., 1963, **130**: 776
- 9 Weinberg S. Phys. Rev., 1965, **137**: B672
- 10 Lurie D, Macfarlane A J. Phys. Rev., 1964, **136**: B816
- 11 Brambilla N, Eidelman S, Heltsley B K et al. Eur. Phys. J. C, 2011, **71**: 1534
- 12 Choi S K et al. (Belle Collaboration). Phys. Rev. Lett., 2003, **91**: 262001
- 13 Tornqvist N A. Phys. Lett. B, 2004, **590**: 209
- 14 Close F E, Page P R. Phys. Lett. B, 2004, **578**: 119
- 15 Wong C Y. Phys. Rev. C, 2004, **69**: 055202
- 16 Braaten E, Kusunoki M. Phys. Rev. D, 2004, **69**: 074005
- 17 Voloshin M B. Phys. Lett. B, 2004, **579**: 316
- 18 Swanson E S. Phys. Lett. B, 2004, **588**: 189

- 19 Swanson E S. Phys. Lett. B, 2004, **598**: 197
- 20 Meng C, Gao Y J, Chao K T. Phys. Rev. D, 2013, **87**: 074035
- 21 Suzuki M. Phys. Rev. D, 2005, **72**: 114013
- 22 Bignamini C, Grinstein B, Piccinini F et al. Phys. Rev. Lett., 2009, **103**: 162001
- 23 Danilkin I V, Simonov Y A. Phys. Rev. Lett., 2010, **105**: 102002
- 24 Prelovsek S, Leskovec L. Phys. Rev. Lett., 2013, **111**: 192001
- 25 Wang P, Wang X G. Phys. Rev. Lett., 2013, **111**: 042002
- 26 Baru V, Epelbaum E, Filin A A et al. Phys. Lett. B, 2013, **726**: 537
- 27 Jansen M, Hammer H W, Jia Y. Phys. Rev. D, 2014, **89**: 014033
- 28 Aaij R et al. (LHCb Collaboration). Nucl. Phys. B, 2014, **886**: 665
- 29 Dong Y, Faessler A, Gutsche T et al. J. Phys. G, 2011, **38**: 015001
- 30 Meng C, Sanz-Cillero J J, Shi M et al. arXiv:hep-ph/1411.3106
- 31 Baru V, Haidenbauer J, Hanhart C et al. Phys. Lett. B, 2004, **586**: 53
- 32 Kaplan D B, Savage M J, Wise M B. Phys. Lett. B, 1998, **424**: 390
- 33 Kaplan D B, Savage M J, Wise M B. Nucl. Phys. B, 1998, **534**: 329
- 34 Cleven M, Guo F K, Hanhart C et al. Eur. Phys. J. A, 2011, **47**: 120
- 35 Ronchen D, Doring M, Huang F et al. Eur. Phys. J. A, 2013, **49**: 44
- 36 Braaten E, Lu M. Phys. Rev. D, 2007, **76**: 094028
- 37 Braaten E, Stapleton J. Phys. Rev. D, 2010, **81**: 014019
- 38 Zhang O, Meng C, Zheng H Q. Phys. Lett. B, 2009, **680**: 453
- 39 Hanhart C, Kalashnikova Y S, Kudryavtsev A E et al. Phys. Rev. D, 2007, **76**: 034007
- 40 Kalashnikova Y S, Nefediev A V. Phys. Rev. D, 2009, **80**: 074004
- 41 Cleven M, Wang Q, Guo F K et al. Phys. Rev. D, 2013, **87**: 074006
- 42 Wang Q, Hanhart C, Zhao Q. Phys. Rev. Lett., 2013, **111**: 132003
- 43 Guo F K, Hanhart C, Meißner U G et al. Phys. Lett. B, 2013, **725**: 127
- 44 Fleming S, Kusunoki M, Mehen T et al. Phys. Rev. D, 2007, **76**: 034006
- 45 Aushev T et al. (Belle Collaboration). Phys. Rev. D, 2010, **81**: 031103
- 46 Aubert B et al. (BaBar Collaboration). Phys. Rev. D, 2008, **77**: 011102
- 47 Beringer J et al. (Particle Data Group Collaboration). Phys. Rev. D, 2012, **86**: 010001
- 48 Aubert B et al. (BaBar Collaboration). Phys. Rev. D, 2008, **77**: 111101
- 49 Adachi I et al. (Belle Collaboration). arXiv:hep-ex/0809.1224
- 50 Meng C, Han H, Chao K T. arXiv:hep-ph/1304.6710